Journal of New Materials for Electrochemical Systems 14, 213-216 (2011)

Fabrication of Nanoporous Copper Ribbons with a Broad Range of Pore Size and Its Application in Lithium-ion Batteries

Jiwei Zheng, Shichao Zhang*, Wenbo Liu, Yalan Xing and Zhijia Du

School of Materials Science and Engineering, Beijing University of Aeronautics and Astronautics, Beijing 100083, China

Received: November 18, 2010, Accepted: April 15, 2011, Available online: July 06, 2011

Abstract: *Nanoporous copper (NPC) ribbons with an average pore size of 5~500nm were fabricated by chemical/electrochemical dealloying of Mn55Cu45 alloy. The influence of different kinds of driving forces on Cu atoms surface diffusivity (Ds), which determines the pore sizes of the resultant NPC, was also systematically investigated. The Ds by chemical dealloying with and without surfactants is about 1.08×10^{-20} $m^2 s^{-1}$ and 1.79×10^{-18} $m^2 s^{-1}$, through which NPC with pore size of ~5nm and ~50nm was produced, while, in electrochemical dealloying with 0 V_{SCE} potential, Ds and pore size increase to 1.16×10^{-15} $m^2 s^{-1}$ and ~500nm respectively. The three dimensional NPC ribbons with the largest pore size (500nm) was chosen as the current collectors to fabricate three dimensional tin thin-film anodes (3D-TTA) with homogeneous tin layers on the ligaments by electroless plating for lithium-ion batteries (LIBs). The 3D-TTA exhibits first discharge capacity of 790 mAh g^{-1}, 45% capacity retention after 10 cycles, indicating a promising application in LIBs.*

Keywords: Nanoporous Copper; Dealloying; Surface Diffusivity; Lithium-ion Batteries

1. INTRODUCTION

Nanoporous metals have drawn great attentions for a wide range of applications in catalysis, sensing, fuel cells and bio-detection due to large surface-to-volume ratios and excellent conductivity. Recently, the most common method to fabricate nanoporous metals is dealloying. Dealloying is a dynamic corrosion and diffusion process during which an element is selectively dissolved, while another remains to produce nanoporous structure. A number of nanoporous metals such as gold, nickel, tungsten, platinum, palladium and copper have been synthesized in this way [1–6]. Among them, nanoporous copper due to a low-cost advantage have attracted many of researchers' interests, such as Raney copper, which is made by dealloying small granules of Al-Cu alloy in NaOH solution [7]. Mn-Cu alloy system, duo to the large standard reversible potential difference (1.477 V) is also used to form nanoporous structures through dealloying. J.R. Hayes et al. [8] synthesized monolithic nanoporous copper with ligaments from 16nm to 125nm by dealloying Mn70Cu30, which exhibits higher than expected yield strength. Lu-Yang Chen et al. [9] systematically investigated the influence of dealloying time on nanoporosity and fabricated nanoporous copper with tunable pore size ranging from 15nm to 150nm from Mn70Cu30 alloy precursor. Nevertheless, there is still a lack of systematic study on the fabrication of NPC with a broader range of pore size for different applications by dealloying Mn-Cu alloy. For example, NPC with smaller pores will be well suited for applications that require greater amounts of surface area, such as hydrogen sensing, while large pores will make NPC possible to be immersed in the deposition solution thoroughly in some deposition process. In this paper, nanoporous copper with a controllable pore size in a broad range from 5nm to 500nm was fabricated by dealloying Mn-Cu system and a clear explanation on the pore size variation mechanism was illustrated. This study will be beneficial to both technological improvement of nano materials fabrication process and the understanding of dealloying process.

Sn and Li can form $Li_{4.4}Sn$ with theoretical capacity of 994 mAh g-1, which has attracted researchers' interests in lithium-ion batteries areas [10-16]. In our previous work, copper foam was chosen as the current collector and three-dimensional tin thin-film anode (3D-TTA) has been prepared by electroless plating. The 3D anode exhibited good capacity volume and cycling performance [17]. NPC, comparing with copper foam, has larger surface-to-volume ratios, which will insure more tin deposition, thus, good perform-

*To whom correspondence should be addressed: Email: csc@buaa.edu.cn
Phone: +86 1082339319

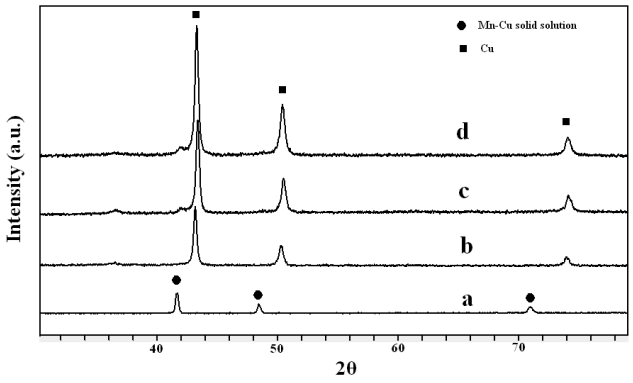

Figure 1. XRD patterns of (a) Mn55Cu45 precursor; (b) NPC by dealloying Mn55Cu45 in 0.075M H_2SO_4 for 4 h; (c) NPC by dealloying Mn55Cu45 in 0.075M H_2SO_4 with sodium dodecyl benzene sulfonate(SDBS) as the surfactants for 17 h; (d) NPC by electrochemically dealloying Mn55Cu45 at 0 V potential for 0.5 h.

ance can be expected. However, there is no research on this emphasis as we known, whereas, this work will be meaningful to broaden the application area of nanoporous metals.

In this article, we have chosen Mn55Cu45 as the precursor for a systematical study on effects of different kinds of driving force on the formation of nanoporous structure through chemical and electrochemical dealloying, and finally fabricated monolithic nanoporous copper with a broad range of pore size. The three dimensional NPC with the largest pore size (500nm) was chosen as the current collector to fabricate 3D-TTA with homogeneous tin layers on the ligaments by electroless plating for promising LIBs applications.

2. EXPERIMENTAL

2.1. Preparation of Mn-Cu alloy precursor

Mn-Cu alloy was prepared from pure Mn (99.99 wt %) and pure Cu (99.999 wt %). Voltaic arc heating was employed to melt the charges in a copper crucible under an argon atmosphere, and then the melt was cooled down into ingots in the crucible. By use of a single roller melt spinning apparatus, the Mn-Cu ingots were remelted in a quartz tube by high-frequency induction heating and then melt-spun onto a copper roller at a circumferential speed of ~3000 rpm in a controlled argon atmosphere. The ribbons obtained were typically 20~40 μm in thickness, 4~6 mm in width, and several centimeters in length.

2.2. Dealloying

All electrolytes in dealloying were made with pure de-ionized water and reagent grade chemicals. Samples were placed directly in the electrolytes for chemical dealloying left for sufficient time for complete dealloying without hydrogengas producing. The electrochemical dealloying was executed by using a PARSTAT@2273 electrochemical workstation in a standard three-electrode cell with the Mn-Cu ribbons served as the work electrode, Pt foil as counter electrode and SCE electrode as the reference electrode. The as-dealloyed samples were rinsed into pure water more than five times to remove the residual chemical substances.

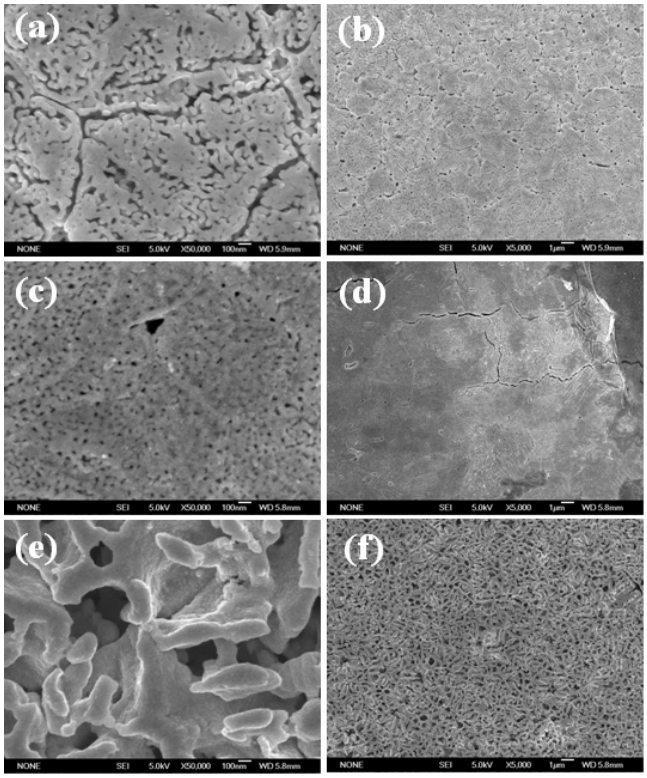

Figure 2. SEM micrographs of NPC by dealloying Mn55Cu45 (a), (b): in 0.075M H_2SO_4 for 4 h; (c), (d): in 0.075M H_2SO_4 adding surfactants for 17 h; (e), (f): at 0 V potential for 0.5 h.

2.3. Preparation of three-dimensional tin thin-film anode

The 3D tin thin-film anodes were prepared by electroless plating tin onto NPC at 45 ℃for 10 min. The plating bath contained 0.1M $SnSO_4$, 1M thiourea, 0.5M sodium hypophosphite and 0.85 M concentrated sulfuric acid.

2.4. Electrochemical charge-discharge behaviours

Electrochemical charge-discharge behaviors were investigated in simulant cells assembled with the as-prepared anode, lithium foil and Celgard 2300 membrane in an Ar-filled glove box. 1M LiPF6/EC-DEC (1:1 by vol.) was used as the electrolytes. All cells were galvanostatically charged and discharged in a battery test system (NEWAREBTS-610, Neware Technology Co., Ltd., China) for a cut-off potential of 0.02~1.5V (vs. Li/Li^+) at ambient temperature.

3. RESULTS AND DISCUSSION

3.1. Fabrication of nanoporous copper with a broad range of pore size

The X-ray diffraction (XRD) pattern shown in Fig. 1 (line (a)) demonstrates that the as-quenched Mn55Cu45 ribbons are a single-phase alloy. Upon dealloying, all the diffraction peaks from the samples with different dealloying conditions can be indexed as an fcc (111), (200), and $(220)_{Cu}$ phase.

We tried a number of acids as the electrolytes to selectively etch

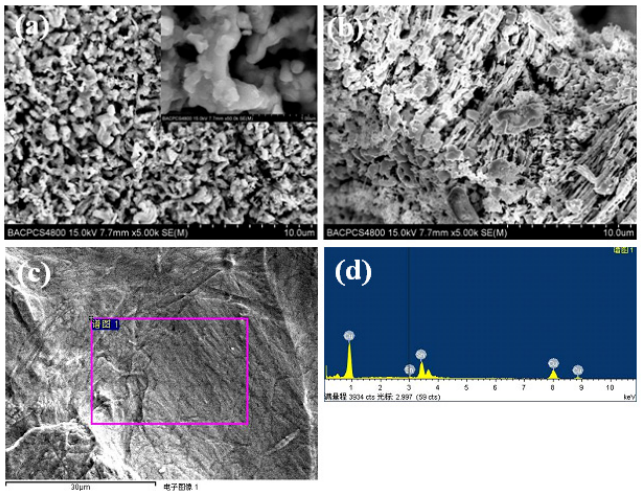

Figure 3. (a), (c): Plan view; (b): cross-sectional SEM micrographs; (d): EDX spectrograms of 3D-TTA.

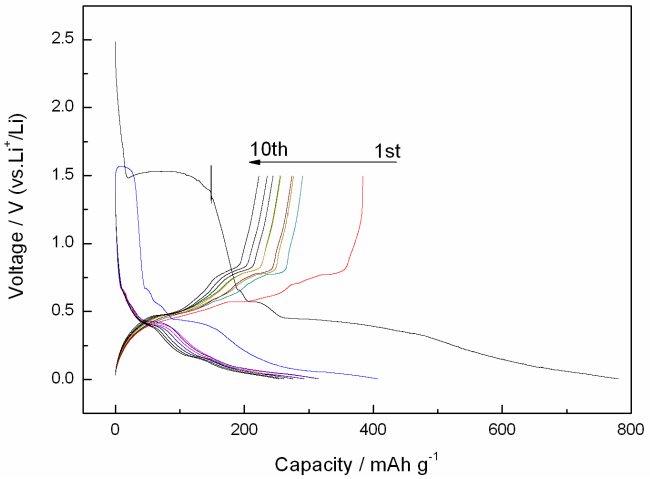

Figure 4. Galvanostatic charge-discharge curves of 3D-TTA at 0.5 C charge–discharge rate.

the rapidly quenched Mn55Cu45 ribbons. It was found that sulphuric acid as well as hydrochloric acid could effectively produce nearly uniform nanoporosity among a certain alloy composition range with suitable acid concentration and dealloying time. In this paper, sulphuric acid rather than hydrochloric acid was chosen as the electrolytes in order to eliminate the influence of Cl^- on surface diffusivity of Cu [18].

Fig. 2 shows SEM micrographs of nanoporous structure of as-dealloyed samples, among which, chemical etching $Mn_{55}Cu_{45}$ thin films with and without surfactants formed nanoporous structure with an average pore size of 5nm and 50nm. Whereas, the pore size of the NPC formed by electrochemically dealloying at 0 V_{SCE} potential for 0.5 h is about 500nm.

It is obvious that different dealloying conditions generated nanoporosity, yet all of the conditions led to significantly different pore sizes. The refinement of nanoporosity and reduction of pore size through chemical dealloying with surfactants are due to partial immobilization of Cu atoms, which hinders surface diffusion of Cu atoms along the alloy/solution interfaces. The similar phenomenon has also occurred in Pd-Ni system. W. C. Li et al. [19] fabricated nanoporous palladium nickel (np-PdNi) with a pore size of 5nm by adding surfactants by dealloying. It has been widely recognized that applied potentials has a significant effect on the sizes of ligaments/pores in nanoporous metals fabricated by electrochemical dealloying [18]. Surface diffusion of more noble elements (Cu) along alloy/solution interfaces has a significant influence on the length scales of ligaments and pores [11, 20]. It is conclusive that 0 V potential herein can markedly enhance the diffusion of Cu atoms and results into the increase of the pore size to 500nm. Previously, H. B. Lu et al. [21] produced nanoporous copper with a pore size of 500nm by electrochemically dealloying Zr38Cu62 at 0.2 V_{SCE} based on the similar mechanism.

It is reported that a maximally unstable spatial period that scales as $d \propto (D_s / V_0)^{\mu}$, where d is the characteristic spacing separated the evolution of Cu clusters, D_S is the surface diffusion coefficient, and V_0 is the velocity of a flat alloy surface with no gold accumulated upon it, μ is a constant, suggested to be 1/6 or 1/4 [11] [22]. Based on the surface diffusion controlled coarsening mechanism, the surface diffusivity (Ds) of Cu atoms along alloy/electrolyte interfaces can be estimated by the equation [22] [24]:

$$D_S = \frac{[d(t)]^4 kT}{32\gamma t\alpha^4}$$

where k is the Boltzmann constant (1.3806×10^{-23} J·K^{-1}), $\gamma$is the surface energy (1.79 J·m^{-2}) [25], $d\ (t)$ is the ligament size at the dealloying time t, α is the lattice parameter of Cu (3.6153×10^{-10} m), and T (293K) is the dealloying temperature. According to the ligament sizes in Table 1, the Ds of Cu atoms were calculated for the dealloying of Mn55Cu45 alloy with different kinds of driving forces, and are also listed in Table 1. It is clearly confirmed the hindering force of surfactants as well as promoting force of voltage to the Cu atoms diffusion, which lead to the formation of smaller pore size (5nm) and larger pore size (500nm).

3.2. NPC for applications in lithium-ion batteries

In order to make nanoporous pores immersed in the deposition solution thoroughly, nanoporous copper with the largest pore size of 500nm was chosen as the current collector. Fig. 3 shows the

Table 1. Correlation between dealloying time and ligament size in NPC for the dealloying of Mn55Cu45 alloy in 0.075M H_2SO_4 at room temperature (293K); the surface diffusivity of Cu atoms along the alloy/electrolyte interface was determined by Eq. (1).

Dealloying methods	Chemical dealloying without suifactants	Chemical dealloying with surfactants	Electrochemical dealloying at 0 V
Dealloying time (t, s)	14400	61200	1800
Ligament size (d(t), nm)	49±1.5	20.7±0.8	146±1.2
Surface diffusivity (Ds, m^{2}s^{-1})	1.79×10^{-18}	1.08×10^{-20}	1.16×10^{-15}

micrographs of 3D tin thin-film anode (3D-TTA). A larger pore size above 1μm was observed after tin deposition, which may be attributed to the effect of coarsening due to 0.85 M concentrated sulfuric acid in the deposition solution and the deposition temperature of 45 ℃ [9]. Simultaneously, a homogeneous tin layer was obtained on the ligaments. The resulted Sn/Cu composites inherited the porosity of the pristine nanoporous copper.

The charge-discharge curves of 3D-TTA shown in Fig. 4 suggest a poor efficiency of 65% during the first cycle with 790mAh g^{-1} initial discharge capacity, which is assigned to the compact microstructure of tin film which severely hinders the lithiation/delithiation process as discussed in our previous report [23]. Besides, the irreversible capacity above 0.8 V is attributed to the formation of solid electrolyte interphase (SEI) layer due to the decomposition of the electrolyte [26]. In the following cycles, charge-discharge curves have the same profile with good cyclability and efficiency.

The good performance of 3D-TTA is attributed to the 3D porous design of the electrode. The porosity provides space to accommodate huge volume change during repeat lithiation/delithiation. Besides, the channels in the electrode facilitate the Li^+ transport while the 3D copper frame effectively functions as electron collector. On the other hand, the volume expansion during discharging might cause shutdown of the connecting windows between the microspores, and thus, would isolate the active material from the electrolyte and hinder the electrochemical lithiation reaction inside the porous electrode [27]. Probably, this shutdown led to a decrease in the utilization of the active material. This is the first time to report that the nanoporous copper was utilized in lithium-ion batteries. The performance could be further improved with the optimization of the nanoporosity performance.

4. CONCLUSION

We fabricated nanoporous copper with a broad range of pore size (5nm~500nm) material through chemical and electrochemical dealloying Mn55Cu45 ribbons. The Cu atoms diffusion rates (Ds) in different dealloying conditions were calculated and compared. The results were used to explain the formation of NPC with a broad range of pore size. The nanoporous copper with the largest pore size of 500nm was used to prepare 3D-TTA with homogeneous tin layer on the ligaments by electroless plating for lithium-ion batteries. The 3D-TTA exhibits first discharge capacity of 790mAh g^{-1}, 45% capacity retention after 10 cycles, indicating a promising application in LIBs.

5. ACKNOWLEDGEMENTS

We give thanks to financial support by the State Key Basic Research Program of PRC (2007CB936502), the National Natural Science Foundation of China (50574008, 50954005, 51074011), the National 863 Program Project (2006AA03Z230, 2008AA03Z208). Also, we are grateful to Prof. T. Zhang and Dr. J.F. Wang for assistance in preparation of the starting alloy ribbons.

REFERENCES

[1] Y. Ding, Y.J. Kim, J. Erlebacher, Adv. Mater., 16, 1897 (2004).
[2] J.K. Chang, S.H. Hsu, I.W. Sun, W.T. Tsai, J. Phys. Chem. C, 112, 1371 (2008).
[3] Z.F. Liu, T. Yamazaki, Y.B. Shen, D. Meng, T. Kikuta, N. Nakatani, T. Kawabata, J. Phys. Chem. C, 112, 1391 (2008).
[4] Y. Ding, A. Mathur, M.W. Chen, J. Erlebacher, Angew. Chem. Int. Ed. 44, 4002 (2005).
[5] J.S. Yu, Y. Ding, C.X. Xu, A. Inoue, T. Sakurai, M.W. Chen, Chem. Mater., 20, 4548 (2008).
[6] J.C. Thorp, K. Sieradzki, L. Tang, P.A. Crozier, A. Misra, M. Nastasi, D. Mitlin, S.T. Picraux, Appl. Phys. Lett., 88, 033110 (2006).
[7] A.J. Smith, T. Tran, M.S. Wainwright, J. Appl. Electrochem., 29, 1085 (1999).
[8] J.R. Hayes, A.M. Hodge, J. Biener, A.V. Hamza, J. Mater. Res., 21, 2611 (2006).
[9] L.Y. Chen, J.S. Yu, T. Fujita, M.W. Chen, Adv. Funct. Mater., 19, 1 (2009)
[10]A.J. Forty, P. Durkin, Philos. Mag, 42, 295 (1980).
[11]J. Erlebacher, M. J. Aziz, A. Karma, N. Dimitrov, K. Sieradzki, Nature, 410, 450 (2001).
[12]W. Choi, J.Y. Lee, B.H. Jung, H.S. Lim, J. Power Sources, 136, 154 (2004).
[13]M. Inaba, T. Uno, A. Tasaka, J. Power Sources, 146, 473 (2005).
[14]H. Morimoto, S. Tobishima, H. Negishi, J. Power Sources, 146, 469 (2005).
[15]L. Balan, R. Schneider, J. Ghanbaja, P. Willmann, D. Billaud, Electrochem. Acta, 51, 3385 (2006).
[16]S.H. Ju, H.C. Jang, Y.C. Kang, J. Power Sources, 189, 163 (2009).
[17]Z. Du, S. Zhang, T. Jiang, Z. Bai, Electrochem. Acta, 55, 3537 (2010).
[18]Z.H. Zhang, Y. Wang, Z. Qi, J.K. Lin, X.F. Bian, J. Phys. Chem. C, 113, 1308 (2009).
[19]W.C. Li and T.J. Balk, Scripta Materialia, 62, 167 (2010).
[20]J. Erlebacher, J. Electrochem. Soc., 151, 614 (2004).
[21]H.B. Lu, Y. Li, F.H. Wang, Scr. Mater., 56, 165 (2007).
[22]L.H. Qian, M.W. Chen, Appl. Phys. Lett., 91, 083105 (2007).
[23]N.A. Gokcen, J. Phase Equilib., 14, 76 (1993).
[24]G. Andreasen, M. Nazzarro, J. Ramirez, R.C. Salvarezza, A.J. Arvia, J. Electrochem. Soc., 143, 466 (1996).
[25]W.R. Tyson, W.A. Miller, Surf. Sci., 62, 267 (1977).
[26]N. Tamura, R. Ohshita, M. Fujimoto, S. Fujitani, M. Kamino, J. Electrochem. Soc., 150, 679 (2003).
[27]J.C. Lytle, H. Yan, N.S. Ergang, W.H. Smyrl, A. Stein, J. Mater. Chem., 14, 1616 (2004).